Kroon, D., Zachos, J.C., and Richter, C. (Eds.)
*Proceedings of the Ocean Drilling Program, Scientific Results* Volume 208

# 5. Data Report: Stable Carbon Isotope Fluctuation of Long-Chain *n*-Alkanes from Leg 208 Hole 1263A across the Paleocene/Eocene Boundary[1]

Takashi Hasegawa,[2] Shinya Yamamoto,[2] and Lisa M. Pratt[3]

## ABSTRACT

Carbon isotope ratios of terrestrial biomarkers extracted from Ocean Drilling Program Hole 1263A show a prominent negative excursion across the Paleocene/Eocene boundary. The isotope profiles of the normal alkanes nonacosane (*n*-$C_{29}$), hentriacontane (*n*-$C_{31}$), and tritriacontane (*n*-$C_{33}$), the first such profiles generated with samples from a pelagic section, are similar to those of carbonate carbon, though the magnitude of the excursion is larger, roughly 4‰–5‰. In addition, the *n*-alkane records show an inflection at 334.70 meters composite depth, which is roughly equivalent to where the inflection occurs in the carbonate record. These results suggest that the terrestrial compounds are directly recording changes in atmospheric carbon $\delta^{13}C$ and that the actual excursion may have been larger than that recorded by marine carbonates.

## INTRODUCTION

The transient thermal maximum event at the Paleocene/Eocene boundary (PETM) is one of the most prominent climatic anomalies in Earth history. Dickens et al. (1995) proposed massive decomposition of methane hydrate as the primary cause of this event, as well as a variety

[1]Hasegawa, T., Yamamoto, S., and Pratt, L.M., 2006. Data report: stable carbon isotope fluctuation of long-chain *n*-alkanes from Leg 208 Hole 1263A across the Paleocene/Eocene boundary. *In* Kroon, D., Zachos, J.C., and Richter, C. (Eds.), *Proc. ODP, Sci. Results,* 208: College Station, TX (Ocean Drilling Program), 1–11. doi:10.2973/odp.proc.sr.208.202.2006
[2]Department of Earth Sciences, Graduate School of Natural Science and Technology, Kanazawa University, Kakuma-machi, Kanazawa 920-1192, Japan. Correspondence author: **jh7ujr@kenroku.kanazawa-u.ac.jp**
[3]Biogeochemical Laboratories, Department of Geological Sciences, Indiana University, 1001 East 10th Street, Bloomington IN 47405-1403, USA.

Initial receipt: 23 August 2005
Acceptance: 11 July 2006
Web publication: 5 December 2006
Ms 208SR-202

of phenomena during the PETM event, including a 2.5‰–3.0‰ negative carbon isotope excursion (CIE). The primary mission of Ocean Drilling Program (ODP) Leg 208 was to recover the PETM so as to constrain the magnitude of the carbon cycle anomaly responsible for the CIE. The boundary was recovered in five of the six sites and is represented by a prominent clay layer at each site. Thickness of the clay layer increases with depth.

The CIE has been documented in both marine (e.g., Kennett and Stott, 1991; Zachos et al., 2003) and terrestrial (e.g., Koch et al., 1992, 1995; Bains et al., 2003; Collinson et al., 2003) sedimentary sections. The magnitude of the excursion, however, is smaller in marine sections, ~3.0‰ compared to 5.0‰ in terrestrial sections (Bowen et al., 2004). Recently, Zachos et al. (2005) provided detailed bulk carbonate carbon isotope stratigraphy across the PETM sequences for five Leg 208 sites (1262, 1263, 1265, 1266, and 1267). They correlated these sequences to the ODP Hole 690B carbon isotope record using several tie points on the basis of inflections in the carbon isotope profiles. Moreover, the magnitude of the excursion as recorded within the clay layer varied as a function of depth, indicating a clear preservational bias.

Organic matter, whether marine or terrestrial, would not be subject to the same preservational biases as carbonate and therefore could provide a more direct signal of the change in atmospheric $\delta^{13}C$. Site 1263 is the shallowest and most complete PETM interval recovered during Leg 208. The Paleocene–Eocene sediments contain minor amounts of extractable long-chain *n*-alkanes with strong odd carbon–number preference derived from leaf wax in terrestrial higher plants (Shipboard Scientific Party, 2004), which provide an opportunity to directly compare the profiles of carbon isotope ratios of inorganic marine carbonate and terrestrial organic carbon using compound-specific carbon isotope analysis on such terrestrial biomarkers.

## METHODS

We sampled 5-cm long quarter-round sections from eight stratigraphic horizons from Sections 208-1263A-33H-2, 33H-CC, and 34X-1 spanning the Paleocene/Eocene (P/E) boundary. The samples were freeze-dried at Kanazawa University (Japan). For samples below Section 208-1263A-34X-1, we freeze-dried three sediments after squeezing pore water on board the ship. The samples were scraped to remove surface contaminants. All 11 samples were ground and extracted with dichloromethane in soxhlet extractors for 48 hr. Each extract was dried under $N_2$ flow, dissolved in 100 mL of hexane, and separated into lipid classes (saturated and unsaturated hydrocarbons, aromatic hydrocarbons, ketones, and polar compounds) by silica gel (deactivated with 5% $H_2O$ w/w) column chromatography.

We analyzed the saturated hydrocarbons using a Hewlett Packard 6890 gas chromatograph (GC) equipped with an on-column injector and flame ionization detector. The first fraction of samples from Core 208-1263A-34X contained unresolved complex mixtures (UCMs) over the region of *n*-alkanes $C_{25}$–$C_{33}$ on gas chromatograms. The urea adduction technique was employed to separate *n*-alkanes from the UCMs. Samples showing no obstructing UCMs for GC isotope ratio mass spectrometry (IRMS) analysis (Fig. F1A, F1B) were not treated. The urea adduction appeared to have no effect on the carbon isotope values of individual *n*-alkanes (Ellis and Fincannon, 1998).

F1. Gas and ion chromatograms, p. 8.

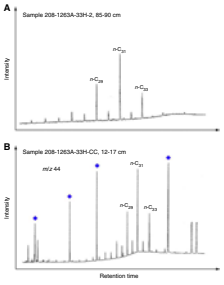

We applied a saturated solution of urea in methanol to the first hydrocarbon fractions dissolved in the hexane:acetone (2:1) mixture. The mixture with white urea precipitate was shaken, settled 1 hr, and centrifuged. We separated the urea precipitate by pipetting the solvent and rinsing the urea three times with clean solvent to completely remove nonadducted materials. We dried the urea crystals under $N_2$ flow and released the adducted compounds by addition of $H_2O$ to the urea crystals. After dissolution of urea in $H_2O$, we added hexane to recover adducted compounds. The solvent including nonadducted compounds was dried under $N_2$, and $H_2O$ was added to dissolve residual urea. Nonadducted compounds were recovered with hexane, and the urea adduction was repeated on the nonadducted compounds to achieve better recovery of *n*-alkanes. See the "Appendix," p. 6, for more information about the urea adduction technique.

We determined the carbon isotope values of *n*-alkanes $C_{29}$ and $C_{31}$ using a GC-IRMS system at Biogeochemical Laboratories, Indiana University. The GC-IRMS system employed a Hewlett Packard 5890 gas chromatograph equipped with a cool on-column injector and interfaced with a Finnigan MAT 252 mass spectrometer by combustion furnace (850°C). Samples were separated on a CP-SIL 8 CB low-breed/MS fused silica capillary column (50 m × 0.32 mm inner diameter with 0.4 mm film thickness). We used helium as carrier gas and programmed the GC oven to heat from 50° to 320°C at 4°C/min, followed by an isothermal hold at 320°C for 25 min. The carbon isotope values for *n*-alkanes $C_{29}$, $C_{31}$, and $C_{33}$ were evaluated by a series of coinjected, deuterated *n*-alkanes of known carbon-isotopic composition ($C_{20}D_{42}$, $C_{24}D_{50}$, and $C_{36}D_{74}$). All carbon isotope ratios ($\delta^{13}C$) are expressed as permil (‰) relative to the Vienna Peedee belemnite (VPDB) standard. Reported isotope ratios represent averaged values of duplicate analyses. Instrumental standard deviation for the analysis (1 σ) is <0.3‰ based on repeated analysis of isotopically known *n*-alkane laboratory standards ($C_{29}$, $C_{31}$, and $C_{33}$).

## DISTRIBUTION OF LONG-CHAIN *N*-ALKANES

Gas chromatograms of the saturated hydrocarbon fraction show remarkable unimodal distribution of *n*-alkanes with strong odd–carbon number preference peaking at *n*-$C_{31}$. The $C_{29}$ *n*-alkane becomes as abundant as *n*-$C_{31}$ below the P/E boundary in Cores 208-1263A-35X, 37X, and 38X. In Cores 208-1263A-33H and 34X, near the P/E boundary, abundances of $C_{29}$, $C_{31}$, and $C_{33}$ dominate over other odd carbon numbers as well as even carbon numbers (Fig. **F1**). The carbon preference index (CPI) for this carbon range varies from 4.9 to 12.5 (Table **T1**). Three samples far below the P/E boundary in the Paleocene section have higher CPI values (8.3, 9.5, and 12.5), whereas samples near the boundary show CPIs of 4.9–7.6. The magnitude of this odd–carbon number preference in *n*-alkane homologs of $C_{29}$–$C_{33}$ is common in epicuticular leaf waxes of terrestrial higher plants (Eglinton and Hamilton, 1967).

**T1.** $\delta^{13}C$ and CPI values, p. 10.

UCMs observed in samples from Core 208-1263A-34X could not be found in deeper horizons to show the extent of obstruction for compound-specific isotope analyses. This indicates that UCMs are not a consequence of thermal maturation. Core 208-1263A-34X was the first core drilled with the extended core barrel system following refusal by the advanced piston corer system. As such, petroleum contamination

from the drill bit might be the source of UCMs. UCMs were effectively removed by urea adduction.

CPI values for the samples from Core 208-1263A-34X, which are as high as those from Core 208-1263A-33H, indicate the consistent origin of *n*-alkanes from terrestrial higher plant waxes, and no substantial contribution of *n*-alkanes from the petroleum contamination is associated with UCMs.

## CARBON ISOTOPE FLUCTUATION OF *N*-ALKANES

The carbon isotope values of the odd carbon–numbered $C_{29}$, $C_{31}$, and $C_{33}$ (Table T1) are plotted vs. meters composite depth (mcd) in Figure F2. There is a constant offset of 0.3‰–0.9‰ between the compounds. Between 378.21 and 335.89 mcd in the upper Paleocene (see Shipboard Scientific Party, 2004, for age-depth model), *n*-$C_{29}$ and *n*-$C_{31}$ gradually decline from –26.6 to –28.1 and –27.2 to –28.5, respectively (Fig. F2), with no change in the offsets. Across the P/E boundary, all *n*-alkanes exhibit abrupt 4‰–5‰ negative shifts. The evaluated *n*-alkanes show nearly identical values in the minimum of the $\delta^{13}C$ excursion at 335.54 mcd. Above this at 335.39 mcd, the values start to recover. A clear inflection is present in the profiles for *n*-$C_{31}$ and *n*-$C_{33}$ between 334.75 and 334.60 mcd. At this level the offset with *n*-$C_{29}$ begins to reappear. This overall pattern is similar to that of the bulk carbonate curve for Holes 1263C and 1263D (Zachos et al., 2005). This suggests that the carbon isotopic composition of these organic compounds directly reflects on changes in atmospheric $CO_2$ across the P/E boundary and that the actual excursion may have been larger than recorded by marine carbonates.

F2. $\delta^{13}C$ profiles, p. 9.

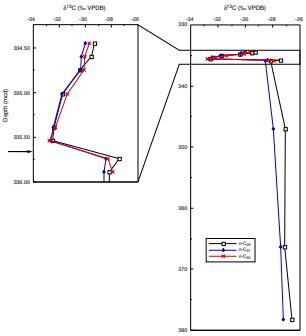

## ACKNOWLEDGMENTS

This research used samples and/or data provided by the Ocean Drilling Program (ODP). ODP is sponsored by the U.S. National Science Foundation (NSF) and participating countries under management of Joint Oceanographic Institutions (JOI), Inc. Jon Fong and Steve Studley of Indiana University assisted with the laboratory work. Funding for this research was provided by Grant-in-aid for Exploratory Research KAKENHI 16654080 by JSPS.

## REFERENCES

Bains, S., Corfield, R.M., and Norris, R.D., 1999. Mechanisms of climate warming at the end of the Paleocene. *Science,* 285(5428):724–727. **doi:10.1126/science.285.5428.724**

Bains, S., Norris, R.D., Corfield, R.M., Bowen, G.J., Gingerich, P.D., and Koch, P.L., 2003. Marine-terrestrial linkages at the Paleocene–Eocene boundary. *In* Wing, S.L. Gingerich, P.D., Schmitz, B., and Thomas, E., (Eds.), *Causes and Consequences of Globally Warm Climates in the Early Paleogene:* Boulder (Geol. Soc. Am.), 1–9.

Bowen, G.J., Beerling, D.J., Koch, P.L., Zachos, J.C., and Quattlebaum, T., 2004. A humid climate state during the Paleocene/Eocene thermal maximum. *Nature (London, U. K.),* 432(7106):495–499. **doi:10.1038/nature03115**

Collinson, M.E., Hooker, J.J., and Grocke, D.R., 2003. Cobham lignite bed and pene-contemporaneous macrofloras of southern England: a record of vegetation and fire across the Paleocene–Eocene Thermal Maximum. *In* Wing, S.L., Gingerich, P.D., Schmitz, B., and Thomas, E., (Eds.), *Causes and Consequences of Globally Warm Climates in the Early Paleogene:* Boulder (Geol. Soc. Am.), 333–349.

Dickens, G.R., O'Neil, J.R., Rea, D.K., and Owen, R.M., 1995. Dissociation of oceanic methane hydrate as a cause of the carbon isotope excursion at the end of the Paleocene. *Paleoceanography,* 10(6):965–972. **doi:10.1029/95PA02087**

Eglinton, G., and Hamilton, R.J., 1967. Leaf epicuticular waxes. *Science,* 156:1322–1335.

Ellis, L., and Fincannon, A.L., 1998. Analytical improvements in irm-GC/MS analyses: advanced techniques in tube furnace design and sample preparation. *Org. Geochem.,* 29(5–7):1101–1117. **doi:10.1016/S0146-6380(98)00157-0**

Kennett, J.P., and Stott, L.D., 1991. Abrupt deep-sea warming, paleoceanographic changes and benthic extinctions at the end of the Palaeocene. *Nature (London, U. K.),* 353(6341):225–229. **doi:10.1038/353225a0**

Koch, P.L., Zachos, J.C., and Dettman, D.L., 1995. Stable isotope stratigraphy and palaeoclimatology of the Palaeogene Bighorn Basin (Wyoming, USA). *Palaeogeogr., Palaeoclimatol., Palaeoecol.,* 115(1–4):61–89. **doi:10.1016/0031-0182(94)00107-J**

Koch, P.L., Zachos, J.C., and Gingerich, P.D., 1992. Correlation between isotope records in marine and continental carbon reservoirs near the Palaeocene/Eocene boundary. *Nature (London, U. K.),* 358:319–322. **doi:10.1038/358319a0**

Shipboard Scientific Party, 2004. Site 1263. *In* Zachos, J.C., Kroon, D., Blum, P., et al., *Proc. ODP, Init. Repts.,* 208: College Station, TX (Ocean Drilling Program), 1–87. **doi:10.2973/odp.proc.ir.208.104.2004**

Zachos, J.C., Wara, M.W., Bohaty, S., Delaney, M.L., Petrizzo, M.R., Brill, A., Bralower, T.J., and Premoli-Silva, I., 2003. A transient rise in tropical sea surface temperature during the Paleocene–Eocene Thermal Maximum. *Science,* 302(5650):1551–1554. **doi:10.1126/science.1090110**

Zachos, J.C., Röhl, U., Schellenberg, S.A., Sluijs, A., Hodell, D.A., Kelly, D.C., Thomas, E., Nicolo, M., Raffi, I., Lourens, L.J., McCarren, H., and Kroon, D., 2005. Rapid acidification of the ocean during the Paleocene–Eocene Thermal Maximum. *Science,* 308(5728):1611–1615. **doi:10.1126/science.1109004**

# APPENDIX

## Confirmation of No Carbon Isotopic Fractionation during Urea Adduction

We applied duplicated urea adduction on samples from Section 208-1263A-34X-1. However, gas chromatograms of nonadducted residues for the samples demonstrated that complete recovery was not achieved during our process (small peaks of targeted *n*-alkanes were observed). Urea adduction should have been repeated until no target peaks in the nonadducted residue were observed. In the case of this study, the amount of each sample extract was limited. Repeated urea adduction might have caused laboratory contamination and/or considerable loss of precious compounds; therefore, we stopped urea adduction after duplication of this process. As long as no isotopic fractionation during the urea adduction process were demonstrated, analytical results from the GC-IRMS system are valuable, even if complete recovery was not achieved. It is generally known that there is no carbon isotopic fractionation during the urea adduction process; however, only limited reports were accessible (Ellis and Fincannon, 1998). Therefore, we tested and vindicated the urea adduction technique employed in this study using standard long-chain alkanes.

### Methods

We used 0.25 µM of pure, commercially produced $C_{28}$ and $C_{32}$ *n*-alkanes as standard materials for each urea adduction. The mixed standards were processed in the same manner as the procedure described in "Methods," p. 2. We omitted repeated adduction on nonadducted residue obtained after the first process in order to test the effect of a single adduction. We performed three experiments independently. Adducted and nonadducted standards for each experiment were injected onto the GC-IRMS system, and we made duplicate analyses. We analyzed original *n*-$C_{28}$ and *n*-$C_{32}$, without any processes, three times. We compared carbon isotope values of initial standards, adducted standards, and nonadducted standards to each other.

### Results

Isotope values for initial standards were determined on the basis of triplicate analyses (Table AT1) to be –32.3‰ for *n*-$C_{28}$ and –27.4‰ for *n*-$C_{32}$. $\delta^{13}C$ values for adducted *n*-$C_{28}$ were 0‰, 0.1‰, and 0.5‰ deviated from the nonadducted values in Experiments A, B, and C, respectively. For *n*-$C_{32}$, Experiment B yielded identical values for the adducted and nonadducted *n*-alkane, whereas Experiment C showed 0.3‰ deviation in the adducted value from the nonadducted value. The averaged magnitude of these deviations is well within the range of instrumental standard deviation (±0.3‰). Average values of the three experiments for adducted *n*-$C_{28}$ and *n*-$C_{32}$ are –32.0‰ and –27.4‰, respectively. The adducted values are 0.3‰ and 0.1‰ deviated positively from initial standard but are still within the range of instrumental standard deviation.

AT1. Urea adduction experiment results, p. 11.

## Discussion and Conclusion

Experiments using long-chain *n*-alkanes *n*-$C_{28}$ and *n*-$C_{32}$ could not show conclusive carbon isotopic fractionation between their adducted and nonadducted statuses. $\delta^{13}C$ values of urea-adducted *n*-alkanes also did not show any considerable fractionation from their untreated status and do not indicate that the urea adduction technique we employed in this study introduced carbon isotope fractionation during the processes. On the basis of this fact and previous knowledge for urea adduction technique (Ellis and Fincannon, 1998), we conclude that our urea adduction technique did not fractionate original carbon isotope values.

**Figure F1. A.** Example of gas chromatogram showing strong odd–carbon number preference with clear peaks. **B.** Example of *m*/*z* 44 ion chromatogram for GC-IRMS analysis. Blue diamonds indicate internal standards for evaluation of carbon isotope values of long-chain *n*-alkanes.

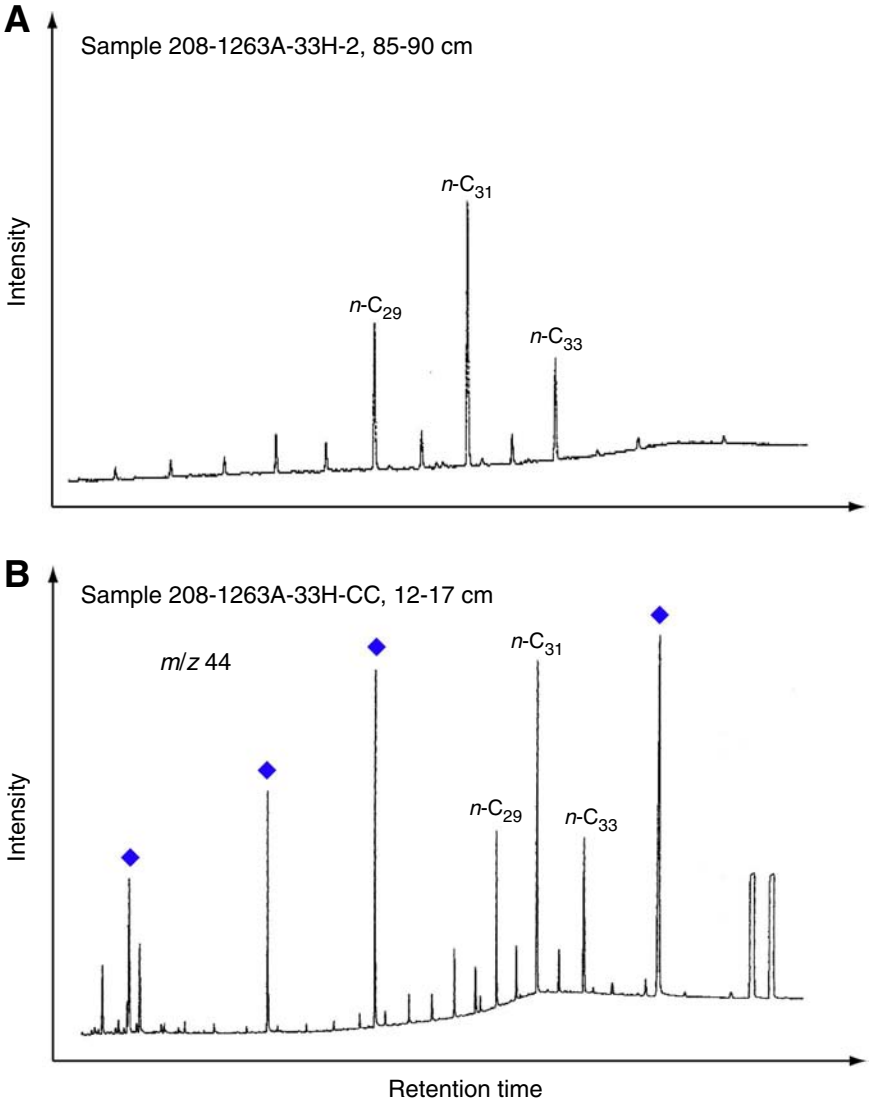

**Figure F2.** Carbon isotope profiles of terrestrial biomarkers. Each long-chain *n*-alkane shows a dramatic negative shift across the Paleocene/Eocene boundary. Arrow indicates lithologic boundary between white carbonate ooze below and dark brown clayey layers above. VPDB = Vienna Peedee belemnite.

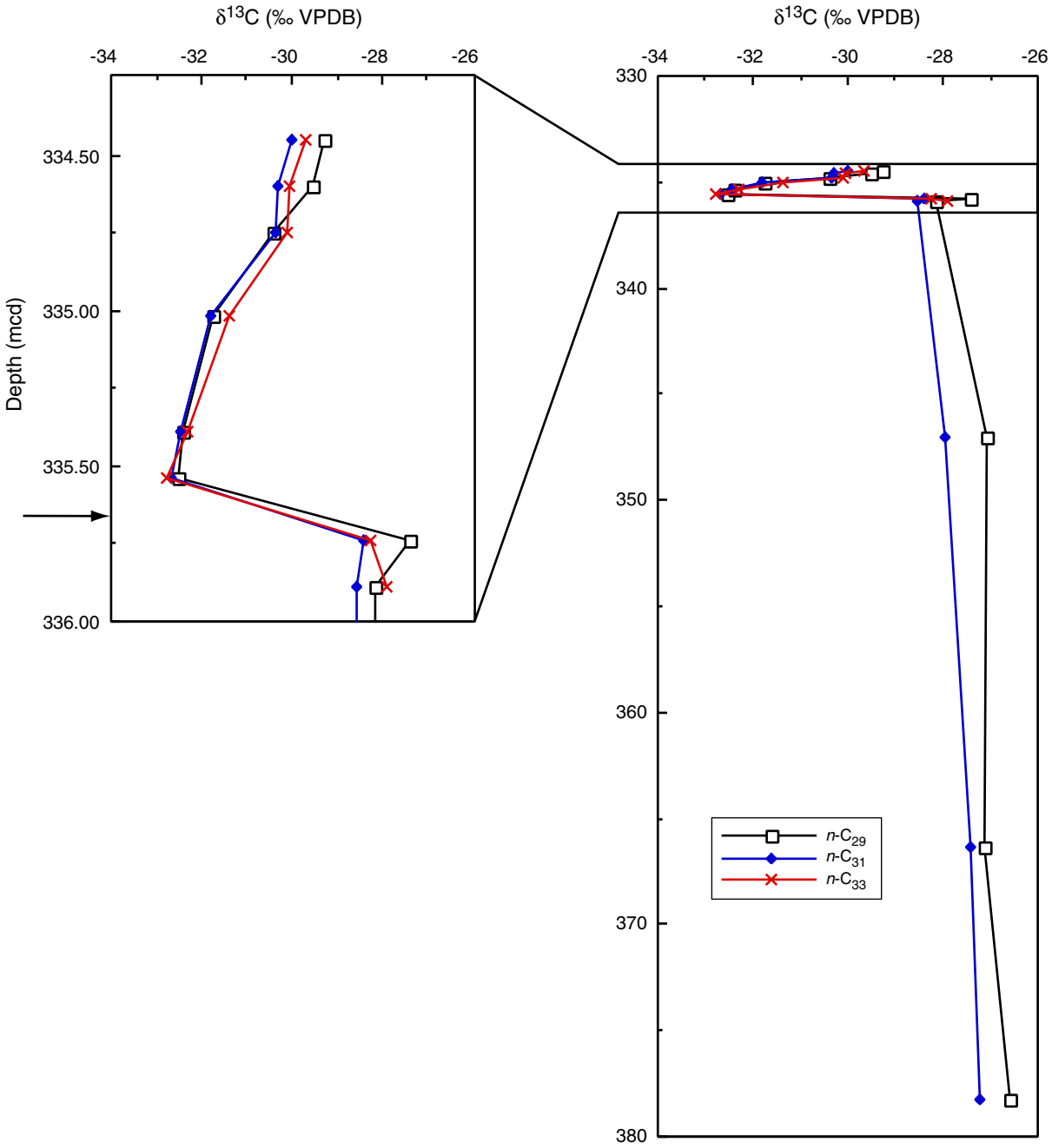

**Table T1.** Carbon isotope values of normal alkanes and CPI values, Hole 1263A.

| Core, section, interval (cm) | Depth (mcd) | $\delta^{13}C$ (‰) | | | |
|---|---|---|---|---|---|
| | | *n*-$C_{29}$ | *n*-$C_{31}$ | *n*-$C_{33}$ | $CPI_{29–33}$ |
| 208-1263A- | | | | | |
| 33H-2, 85–90 | 334.45 | –29.3 | –30.0 | –29.7 | 6.7 |
| 33H-2, 100–105 | 334.6 | –29.5 | –30.3 | –30.0 | 5.5 |
| 33H-2, 115–120 | 334.75 | –30.4 | –30.3 | –30.1 | 4.9 |
| 33H-CC, 12–17 | 335.02 | –31.7 | –31.8 | –31.4 | 5.4 |
| 34X-1, 5–10 | 335.39 | –32.4 | –32.5 | –32.3 | 6.1 |
| 34X-1, 20–25 | 335.54 | –32.5 | –32.7 | –32.8 | 5.6 |
| 34X-1, 40–45 | 335.74 | –27.4 | –28.4 | –28.3 | 7.6 |
| 34X-1, 55–60 | 335.89 | –28.1 | –28.5 | –27.9 | 7.0 |
| 35X-3, 140–150 | 347.06 | –27.1 | –27.9 | ND | 12.5 |
| 37X-3, 90–100 | 366.38 | –27.1 | –27.4 | ND | 8.3 |
| 38X-3, 140–150 | 378.21 | –26.6 | –27.2 | ND | 9.0 |

Notes: Each isotope value represents average for duplicate analyses. Depth is at top horizon of the sample. Carbon preference index $(CPI)_{29–33} = 0.5 \times \Sigma_{29,\ 31,\ 33}(1/\Sigma C_{28,\ 30,\ 32} + 1/\Sigma C_{30,\ 32,\ 34})$. ND = not determined.

**Table AT1.** Urea adduction experiment results.

| Experiment | Material | | $\delta^{13}C$ (‰ VPDB) | |
|---|---|---|---|---|
| | | | *n*-$C_{28}$ | *n*-$C_{32}$ |
| Initial standards | | | –32.2 | –27.1 |
| | | | –32.5 | –27.5 |
| | | | –32.1 | –27.6 |
| | | Average | –32.3 | –27.4 |
| | | Standard deviation | 0.2 | 0.2 |
| Experiment A | Adducted | | –32.1 | –27.6 |
| | | | –31.8 | –27.6 |
| | | Average | –31.9 | –27.6 |
| | | Nonadduct | –31.8 | ND |
| | | | –32.1 | ND |
| | | Average | –31.9 | |
| Experiment B | Adducted | | –32.2 | –27.4 |
| | | | –32.2 | –27.3 |
| | | Average | –32.2 | –27.3 |
| | Nonadduct | | –32.4 | –27.4 |
| | | | –32.3 | –27.2 |
| | | Average | –32.3 | –27.3 |
| Experiment C | Adducted | | –31.9 | –27.1 |
| | | | –31.8 | –27.4 |
| | | Average | –31.8 | –27.2 |
| | Nonadduct | | –32.3 | –27.5 |
| | | | ND | –27.5 |
| | | Average | –32.3 | –27.5 |

Notes: Each isotope value (except for average) represents a single run. VPDB = Vienna Peedee belemnite. ND = not determined (peaks were not large or small enough to evaluate).